ELSEVIER

Progress in Biophysics & Molecular Biology 85 (2004) 387–405

Progress in Biophysics & Molecular Biology

www.elsevier.com/locate/pbiomolbio

Development of models of active ion transport for whole-cell modelling: cardiac sodium–potassium pump as a case study

N.P. Smith[a,*], E.J. Crampin[a,b,c,1]

[a] *Bioengineering Institute, The University of Auckland, Private Bag 92019, Auckland, New Zealand*
[b] *Centre for Mathematical Biology, Mathematical Institute, 24-29 St Giles', Oxford OX1 3LB, UK*
[c] *University Laboratory of Physiology, Parks Road, Oxford OX1 3PT, UK*

Abstract

This study presents a method for the reduction of biophysically-based kinetic models for the active transport of ions. A lumping scheme is presented which exploits the differences in timescales associated with fast and slow transitions between model states, while maintaining the thermodynamic properties of the model. The goal of this approach is to contribute to modelling of the effects of disturbances to metabolism, associated with ischaemic heart disease, on cardiac cell function.

The approach is illustrated for the sodium-potassium pump in the myocyte. The lumping scheme is applied to produce a 4-state representation from the detailed 15-state model of Läuger and Apell, Eur. Biophys. J. 13 (1986) 309, for which the principles of free energy transduction are used to link the free energy released from ATP hydrolysis (ΔG_{ATP}) to the transition rates between states of the model. An iterative minimisation algorithm is implemented to determine the transition rate parameters based on the model fit to experimental data. Finally, the relationship between ΔG_{ATP} and pump cycling direction is investigated and compared with recent experimental findings.

Keywords: Sodium–potassium pump; Na/K-ATPase; Free energy transduction; Cardiac myocyte metabolism; Mathematical model

1. Introduction

Over the last 40 years mathematical modelling has provided an increasingly important tool for representing and understanding many of the fundamental mechanisms and processes relevant to single-cell myocyte electrophysiology and, in combination with spatially distributed continuum

*Corresponding author. Tel.: +64-93737599x84720; fax: +64-93677157.
E-mail addresses: np.smith@auckland.ac.nz (N.P. Smith), e.crampin@auckland.ac.nz (E.J. Crampin).
[1] Authors contributed equally.

0079-6107/$ - see front matter © 2004 Elsevier Ltd. All rights reserved.
doi:10.1016/j.pbiomolbio.2004.01.010

techniques, cardiac tissue excitation. During this time a number of modelling frameworks have been developed to encompass new understandings gained from the iteration between experimental and modelling studies. Two recent examples of electrophysiological modelling frameworks are the models of Noble et al. (1998) and Luo and Rudy (1994a,b). These models, which have had considerable successes in elucidating the mechanisms underlying the cardiac action potential (Noble and Rudy, 2001), consist of representations of the various ion currents, pumps and exchangers which have been experimentally characterised, along with explicit accounting for ion flow between cellular subdomains such as the sarcoplasmic reticulum and diadic space.

The contribution of active ion transport to the development of the action potential has been well established in cell modelling. A simple model of the sodium–potassium pump motivated by energetic principles has previously been proposed for cardiac cells by Chapman et al. (1979) to demonstrate the importance of electrogenic active transport to the transmembrane current (Johnson et al., 1980). The requirement for thermodynamic consistency, however, has not, in general, been adopted for whole-cell modelling. In part, this is because until recently the metabolic regulation of myocyte electrophysiology has received little attention in whole-cell models, despite its obvious importance in understanding pathologies such as ischaemia, where blood supply to the heart muscle is reduced (although see Ch'en et al., 1998, for progress towards incorporating these biochemical processes in a heart cell model). This means that, in general, the models are not well posed for incorporating metabolite dependence into their parameters. This point is demonstrated by investigating the equations used in the Noble and Luo-Rudy models to govern the rate of the sodium–potassium pump: despite the fact that this process is electrogenic and is dependent on the free energy of ATP hydrolysis, the equations in both models are independent of metabolite concentration and, in the case of the Noble model, also independent of membrane potential.

Whole-cell electrophysiology models have benefited greatly from patch-clamp based measurement techniques which can provide detailed kinetic data for individual ion channels and transporters. The empirical functions and parameters are, in general, fitted from data obtained under normal physiological conditions (or under conditions as close to normal as possible) where ATP concentration, and the free energy change associated with ATP hydrolysis, remain approximately constant. Recent results from Jansen et al. (2003) demonstrate that under pathophysiological conditions such as myocardial ischaemia the drop in free energy may cause the sodium–potassium pump to stop or reverse. These data are incompatible with such models, which will always give a positive pump current for the reason that they are not formulated to be consistent with the fundamental principles of free energy transduction (Hill, 1989). Thus, if we are to employ the modelling approach to understand mechanisms underlying such cellular pathologies, the formulations of these model components need to be revised.

In this report we present a methodology for the development of models of ion transporters which are energetically consistent and which may therefore be coupled to the metabolic processes occurring in the cell. Taking as a specific example the sodium–potassium pump in the cardiac myocyte, we develop the traditional model construction to show how the different timescales in the underlying molecular processes can be used to reduce model complexity. This is motivated by the need to maximise the advantages of biophysically based modelling while minimising computational complexity. Our goal is to produce a model of the sodium–potassium pump which can be used as a component in the whole-cell myocyte modelling frameworks of Noble et al. (1998) and Luo and Rudy (1994a,b) to predict pump function and, with additions and similar

modifications to other model components, ultimately whole myocyte behaviour when cellular metabolism is compromised.

2. Cardiac Na/K-ATPase

The sodium–potassium pump (Na/K-ATPase) is one of the principal sarcolemmal ion transporters and is present in nearly all mammalian cell membranes. Its major function is to keep the intracellular sodium concentration low and intracellular potassium high so as to maintain large gradients in concentrations of these ions across the cell membrane. The sodium–potassium pump couples Na^+ and K^+ transport against their electrochemical gradients to the hydrolysis of ATP, which provides the free energy required for the pump. The metabolic cost of maintaining the gradients is significant: the pump typically consumes some 17% of the total cellular ATP turnover (Schramm et al., 1994). There is a tight coupling between the extrusion of three sodium ions and the import of two potassium ions for each ATP molecule hydrolysed (Glitsch, 2001). The net transport of one positive charge out of the cell for each ATP hydrolysed, i.e., for each pump cycle, contributes a net outward transmembrane current under normal conditions. Thus the net reaction for the pump cycle is

$$\mathrm{ATP} + 3\mathrm{Na}_i^+ + 2\mathrm{K}_e^+ \rightleftharpoons \mathrm{ADP} + \mathrm{Pi} + 3\mathrm{Na}_e^+ + 2\mathrm{K}_i^+, \tag{1}$$

where the subscripts i and e represent intra- and extracellular ion pools, respectively. The relationship between the free energy of ATP hydrolysis and work performed against these gradients (quantified in Section 2.2) determines the reversal condition for the pump current.

Sodium and potassium gradients are involved in numerous processes, including maintaining membrane potential, regulation of cell volume and sodium- and potassium-coupled secondary transport of other ions and molecules, coupled to movement of Na^+ or K^+ down their electrochemical gradients. In particular, in heart cells (and other electrically excitable cell types) where rapid Na^+ influx generates the up-stroke of the action potential, the sodium–potassium pump extrudes the majority of the Na^+ which enters the cell during each cycle. The clinical implications of reduced Na/K-ATPase velocity in ischaemia are pronounced. The reduction of free energy available from ATP hydrolysis results in an accumulation of intracellular sodium ions (Jansen et al., 2003) and may lead to rising cytoplasmic calcium concentration (due to reduced Na/Ca exchanger activity) and a drop in pH (via reduced Na/H exchange, Ingwall, 2002), disrupting regulation of cell volume and intracellular calcium handling. Thus the maintenance of Na/K-ATPase activity is critical to the survival and recovery of the myocyte during and after ischaemia.

2.1. Kinetic models

The Na/K-ATPase, first described by Skou in 1957, is now recognised as being one member of a large protein family: the P-type active cation transporters (see for example the P-type ATPase Database[2]), which also includes H/K-ATPases and Ca-ATPases including the sarcoplasmic

[2] http://biobase.dk/~axe/Patbase.html.

reticulum Ca-ATPase (SERCA). Structures for the Ca-ATPase are now becoming available (Toyoshima et al., 2000). These new protein structure data are providing insights into the mechanism of the catalytic pump cycle. However, long before these structural data were available, detailed kinetic models of the different functional states which comprise the pump cycle have been proposed, based on extensive kinetic characterisations. The Post-Albers model for ATP-coupled Na/K transport (Apell, 1989) represents a consensus view of the mechanism, as currently understood. Na/K-ATPase enzyme can exist in two major conformational states; one of which preferentially binds Na^+ and ATP, and the other which has higher affinity for K^+ and inorganic phosphate. ATP binding facilitates the conformational change between these states.

The Post-Albers scheme is a consecutive (“ping-pong”) mechanism for the kinetics of ion translocation (Fell, 1997), which supposes that the enzyme may bind to only one species of ion (either K^+ or Na^+) at a given time, moving between two different enzyme conformations. Many intermediate enzyme complexes and partial reaction steps have been proposed, however, the basic mechanism of the Post-Albers cycle (illustrated in Fig. 1) is as follows. Of the two conformational states of the enzyme, E_i preferentially binds Na^+ on the cytoplasmic side and E_e exposes cation binding sites to the extracellular side and has higher affinity for K^+. Intracellular ATP binds preferentially to the enzyme in the E_e conformation to facilitate inward transport of two K^+ ions via conformational transition to the E_i state. Hydrolysis of ATP and concomitant phosphorylation of the enzyme when Na^+ is bound to the cytoplasmic-facing binding sites of E_i leads to the transition of the phosphorylated protein back to the extracellular conformation, resulting in the

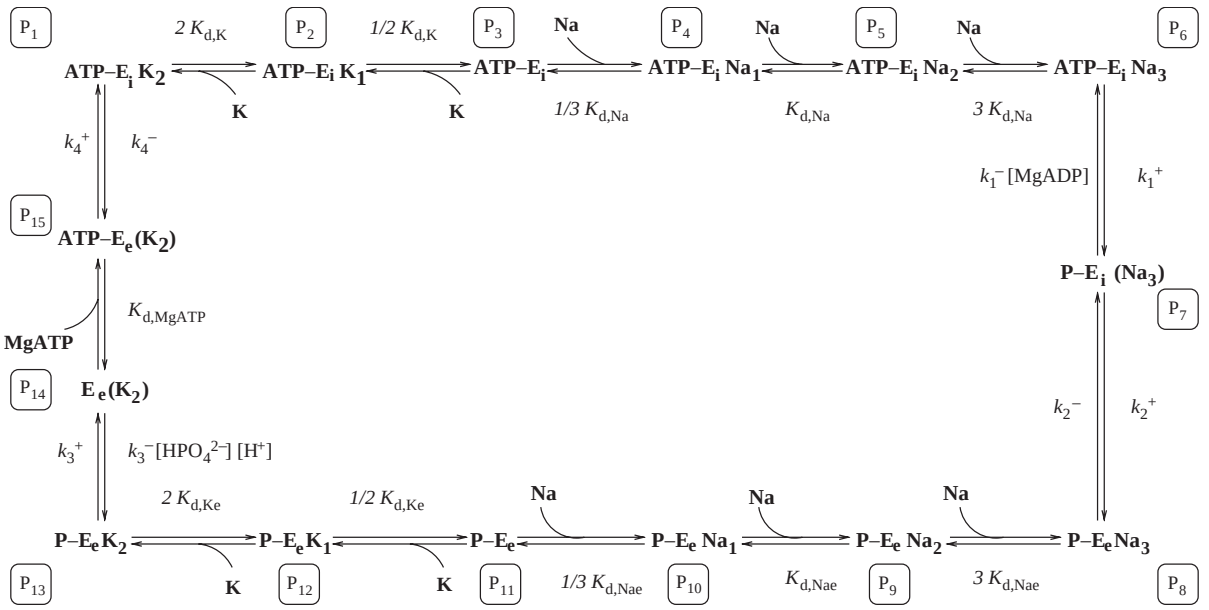

Fig. 1. The 15-state Post-Albers reaction cycle for the sodium–potassium pump ($P_1, \ldots, P_{15}$). E, P-E and ATP-E represent the native, phosphorylated and ATP-bound enzyme, respectively, and the subscripts i and e denote conformations in which cation binding sites are exposed to the cytosol and extracellular medium, respectively. Ion binding sites are assumed to be identical, so that the mth ion binding to one of n identical binding sites has dissociation constant $mK_d/(n-m+1)$, where K_d is the dissociation constant for a single ion-binding site interaction. Forward cycling, indicated by the rate constants k_j^+, is taken to be clockwise.

outward transport of three Na^+ ions. A key mechanism which efficiently couples the free energy of ATP hydrolysis to ion transport is the 'occlusion' of bound Na^+ and K^+ ions accompanying phosphorylation and dephosphorylation of the protein, respectively, preventing wastage via the unbinding of ions before conformational change is effected ('slippage'). This tight coupling between conformational change and the binding of ions, results in the strict $3Na^+$:$2K^+$ stoichiometry per ATP hydrolysed.

Several of the reaction steps, demarcated in Fig. 1 by dissociation constants, K_d, rather than forward and backward rate constants, are assumed to be rapid reactions. These include the ion binding and unbinding reactions, as well as the binding of MgATP. The consequences of these rapid equilibrium assumptions for simplification of the kinetics are explored below in Section 3. Note, however, that the steps involving the conformational change (E_i to E_e and vice versa), as well as several other reaction steps involving metabolites, are not considered to be in rapid equilibrium. The further simplification has also been made that the three Na^+ binding sites are identical and independent, as are the two K^+ sites (Apell, 1989), and so each can be written in terms of a characteristic single-ion dissociation constant K_d. While this approximation simplifies the algebra below considerably, it is not a requirement for the analysis of the model that follows.

Finally, we will assume that ATP hydrolysis follows the reaction

$$\mathrm{MgATP} + \mathrm{H_2O} \rightleftharpoons \mathrm{MgADP} + \mathrm{Pi} + \mathrm{H^+} \tag{2}$$

with equilibrium constant $K_{\sim \mathrm{MgATP}}$. Explicit accounting for proton concentration allows us to track the effects of pH changes accompanying ischaemia (Huang and Askari, 1984). We do not differentiate between different forms of inorganic phosphate, Pi, (but see Eq. (33) below), and so $K_{\sim \mathrm{MgATP}}$ must be treated as an apparent equilibrium constant. Note, however, that we are assuming the dominant buffering of ATP is in the form of MgATP and other ATP-bound species have been ignored (Gupta et al., 1978).

2.2. Thermodynamic considerations

Fundamental to predicting the direction of the sodium–potassium pump in the ischaemic myocyte is the coupling of the free energy released by the hydrolysis of ATP ($\Delta G_{\sim \mathrm{MgATP}}$) to the energy consumed for each pump cycle ΔG_{pump} in transporting 2 K^+ ions into the cell and 3 Na^+ ions out of the cell. $\Delta G_{\sim \mathrm{MgATP}}$ is determined from the ratio of the concentrations of MgATP to its hydrolysis products:

$$\Delta G_{\sim \mathrm{MgATP}} = \Delta G^o_{\sim \mathrm{MgATP}} + RT \ln \frac{[\mathrm{MgADP}][\mathrm{Pi}][\mathrm{H^+}]}{[\mathrm{MgATP}]}, \tag{3}$$

where T is absolute temperature, R is the universal gas constant and $\Delta G^o_{\sim \mathrm{MgATP}}$, the free energy under standard conditions, is related to the equilibrium constant for the hydrolysis reaction according to

$$\Delta G^o_{\sim \mathrm{MgATP}} = -RT \ln K_{\sim \mathrm{MgATP}}. \tag{4}$$

Note that under normal physiological conditions in the heart, $\Delta G_{\sim \mathrm{MgATP}}$ is negative (approximately -58 kJ mol^{-1}, Ingwall, 2002) meaning ATP hydrolysis is exergonic or energy releasing.

The energy required per pump cycle, ΔG_{pump}, is the sum of work done in transporting the ions against their electrochemical gradients. The energy required to translocate a K^+ ion from the extracellular environment to the intracellular cytosol is the sum of two terms:

$$\Delta G_{\text{K}} = RT \ln \frac{[\text{K}_\text{i}^+]}{[\text{K}_\text{e}^+]} + FV_\text{m}, \tag{5}$$

where F is Faraday's constant. The first term accounts for the movement of a potassium ion against its concentration gradient and the second for movement of a charge through the membrane potential V_m (approximately -85 mV in the myocyte). The equivalent expression for translocation of a single Na^+ ion is given by:

$$\Delta G_{\text{Na}} = RT \ln \frac{[\text{Na}_\text{e}^+]}{[\text{Na}_\text{i}^+]} - FV_\text{m}. \tag{6}$$

ΔG_{pump} can now be determined from the quantities calculated in Eqs. (5) and (6) and the pump stoichiometry: $\Delta G_{\text{pump}} = 2\Delta G_{\text{K}} + 3\Delta G_{\text{Na}}$. The pump current direction can be determined on purely thermodynamic grounds, according to the second law. When $-\Delta G_{\sim \text{MgATP}} > \Delta G_{\text{pump}}$, as under normal physiological conditions, the pump runs in the forward direction; Na^+ is extruded and K^+ is transported into the cell (with net outward current flow). If the free energy of hydrolysis of ATP drops, such that at $\Delta G_{\sim \text{MgATP}} + \Delta G_{\text{pump}} = 0$, the pump will be in equilibrium and the net transport of ions will cease. Should the total free energy change become negative, the pump cycle reverses, using the ionic electrochemical gradients to generate ATP from ADP and Pi. Reversal of the sodium–potassium pump has been reported for erythrocytes (red blood cells, Glynn and Lew, 1970; Lew et al., 1970) by manipulation of ion and metabolite concentrations to unphysiological levels. More recently, experiments in cardiac Purkinje cells (Glitsch and Tappe, 1995) have shown the dependence of the reversal potential for the pump on $\Delta G_{\sim \text{MgATP}}$ while maintaining constant ionic gradients across the membrane. These thermodynamic considerations indicate the point at which the pump reverses and the current changes sign, however, the rate of the reaction is dependent on the kinetic parameters and so may be negligible if one or more of the partial reaction steps are essentially irreversible.

Following Hill (1989), an examination of the reaction at thermodynamic equilibrium reveals a thermodynamic constraint on the kinetic parameters for the scheme shown in Fig. 1. As stated above, at equilibrium the net transport around the cycle will be zero, or equivalently, each partial reaction obeys detailed balance; the forward transition rate will be equal to the backward transition rate for each partial reaction step:

$$k_i^+ P_i = k_i^- P_{i+1}, \tag{7}$$

where P_i and P_{i+1} are the fractional occupancies of adjacent states and $k_i^\pm$ are (pseudo) first-order rate constants. Multiplying each of these expressions, for an n-step cycle

$$\prod_{i=1}^{n} k_i^+ P_i = \prod_{i=1}^{n} k_i^- P_{i+1}, \tag{8}$$

where $P_{n+1} \equiv P_1$, reveals that the kinetic parameters are not independent. Because the state occupancies cancel in this expression, this constraint for the kinetic parameters must hold whether or not the system is at equilibrium.

For transitions in which ions bind or unbind from the enzyme this expression can be written explicitly in terms of higher order rate constants and reactant concentrations, for example the equivalent expression when state transition between i and $i+1$ involves the binding of an ion with concentration [Y] is written as

$$k_i^+[\mathrm{Y}]P_i = k_i^- P_{i+1}, \tag{9}$$

where in this case k_i^+ is a second-order rate constant. We can now multiply expressions for each transition around the state diagram in Fig. 1 to show that at equilibrium

$$\frac{k_1^+k_2^+k_3^+k_4^+K_{\mathrm{d},K_\mathrm{i}}^2K_{\mathrm{d},Na_\mathrm{e}}^3}{k_1^-k_2^-k_3^-k_4^-K_{\mathrm{d,MgATP}}K_{\mathrm{d},K_\mathrm{e}}^2K_{\mathrm{d},Na_\mathrm{i}}^3} = \frac{[\mathrm{MgADP}][\mathrm{Pi}][\mathrm{H}^+][\mathrm{K_i}]^2[\mathrm{Na_e}]^3}{[\mathrm{MgATP}][\mathrm{K_e}]^2[\mathrm{Na_i}]^3}. \tag{10}$$

Now at equilibrium $\Delta G_{\sim\mathrm{MgATP}} + \Delta G_{\mathrm{pump}} = 0$, or

$$-\ln K_{\sim\mathrm{MgATP}} + \ln\frac{[\mathrm{MgADP}][\mathrm{Pi}][\mathrm{H}^+]}{[\mathrm{MgATP}]} + 3\ln\frac{[\mathrm{Na_e}]}{[\mathrm{Na_i}]} + 2\ln\frac{[\mathrm{K_i}]}{[\mathrm{K_e}]} - \frac{FV_\mathrm{m}}{RT} = 0$$

which can be rearranged to show that at equilibrium (Tanford, 1981)

$$\frac{[\mathrm{MgADP}][\mathrm{Pi}][\mathrm{H}^+][\mathrm{K_i}]^2[\mathrm{Na_e}]^3}{[\mathrm{MgATP}][\mathrm{K_e}]^2[\mathrm{Na_i}]^3} = K_{\sim\mathrm{MgATP}}\,\mathrm{e}^{FV_\mathrm{m}/RT}. \tag{11}$$

Thus, combining Eqs. (10) and (11), the voltage dependence of the transition rates must be such that

$$\frac{k_1^+k_2^+k_3^+k_4^+K_{\mathrm{d},K_\mathrm{i}}^2K_{\mathrm{d},Na_\mathrm{e}}^3}{k_1^-k_2^-k_3^-k_4^-K_{\mathrm{d,MgATP}}K_{\mathrm{d},K_\mathrm{e}}^2K_{\mathrm{d},Na_\mathrm{i}}^3} = K_{\sim\mathrm{MgATP}}\,\mathrm{e}^{FV_\mathrm{m}/RT}. \tag{12}$$

In the specific context of the sodium–potassium pump in the myocyte two important points warrant discussion. The first is the assumption that only one thermodynamic cycle exists and that there are no transitions between states not linked in Fig. 1 or, alternatively, that there is no mechanism for 'slippage', as discussed above. Such cycles would provide a mechanism for dissipating free energy independent of ion transport and potentially give a changed, or even variable, stoichiometry. Thus a corollary of this assumption is that for every MgATP molecule hydrolysed three Na^+ ions and two K^+ ions are transported across the cell membrane. The characterisation of the pump as a single unbranched kinetic cycle is supported by the well-established voltage independent stoichiometry of the pump (Glitsch, 2001), discussed in Section 2.1. It is also supported by experimental data (Jansen et al., 2003) showing that the pump operates in the forward direction when $\Delta G_{\sim\mathrm{MgATP}} + \Delta G_{\mathrm{pump}}$ is only just less than zero, strongly implying that any flux through alternative, free energy-dissipating biochemical cycles is minimal relative to the net rate of ion transport.

The second point relates to the form of the voltage dependence of the state transitions. Equation (12) constrains the transition rates but provides no information on the likely location of a voltage-dependent transition step or steps. A number of studies suggest that the voltage dependence is contained within the sodium transport function of the pump (De Weer et al., 1988; Rakowski et al., 1997) and is most likely to affect the release (or re-binding) of Na^+ ions to the extracellular space (Apell, 1989). This evidence justifies the separation of Eq. (12) into a

constraint

$$\frac{k_1^+ k_2^+ k_3^+ k_4^+ K_{\mathrm{d},K_\mathrm{i}}^2 \left(K_{\mathrm{d},Na_\mathrm{e}}^0\right)^3}{k_1^- k_2^- k_3^- k_4^- K_{\mathrm{d,MgATP}} K_{\mathrm{d},K_\mathrm{e}}^2 \left(K_{\mathrm{d},Na_\mathrm{i}}^0\right)^3} = K_{\sim \mathrm{MgATP}} \tag{13}$$

while partitioning the voltage dependence of the sodium dissociation reactions as follows

$$K_{\mathrm{d},Na_\mathrm{e}} = K_{\mathrm{d},Na_\mathrm{e}}^0 \mathrm{e}^{(1+\Delta)FV_\mathrm{m}/3RT}, \qquad K_{\mathrm{d},Na_\mathrm{i}} = K_{\mathrm{d},Na_\mathrm{i}}^0 \mathrm{e}^{\Delta FV_\mathrm{m}/3RT}, \tag{14}$$

where $K_{\mathrm{d},Na_\mathrm{i}}^0$ and $K_{\mathrm{d},Na_\mathrm{e}}^0$ are the Na^+ dissociation constants at $V_\mathrm{m} = 0$ and the factor Δ determines how the voltage dependence is partitioned between the intra- and extracellular Na^+ dissociation reactions.

3. Kinetic considerations: model reduction

Deterministic kinetic models for enzyme activity assume a reaction scheme consisting of a number of partial reactions, which represents average molecular behaviour over large times, or for large populations of molecules. The properties of the kinetic model are determined by the rates at which the partial reactions take place. Often it is possible to reduce the complexity, that is, to reduce the number of dependent variables in the reaction scheme, by observing that several processes occur on timescales which are much faster than others in the model. In this section we will investigate how the rapid equilibrium assumption for certain partial reaction steps can be used to reduce the number of enzyme states which must be considered, by exploiting these differences in timescales.

3.1. Lumping schemes for rapid equilibrium partial reactions

We use the following example to show how the assumption of rapid equilibrium for certain partial reactions, or reaction steps, leads to a simplified representation of the kinetics by use of a lumping scheme which reduces the number of variables. Three reaction steps are shown between four reaction intermediates, $X_1, \ldots, X_4$:

$$\cdots X_1 \underset{k_1^-}{\overset{k_1^+}{\rightleftharpoons}} X_2 \underset{k_2^-}{\overset{k_2^+}{\rightleftharpoons}} X_3 \underset{k_3^-}{\overset{k_3^+}{\rightleftharpoons}} X_4 \cdots .$$

Let us assume that the middle reaction, between X_2 and X_3, is very fast relative to the other reaction steps,

$$k_2^+, k_2^- \gg k_1^+, k_1^-, k_3^+, k_3^-, \ldots \tag{15}$$

so that X_2 and X_3 are in rapid equilibrium with each other

$$X_3(t) = K_2 X_2(t), \tag{16}$$

where $K_2 = k_2^+/k_2^-$ is the equilibrium constant for the reaction step. Defining a new variable X_{23}

$$\begin{aligned} X_{23}(t) &= X_2(t) + X_3(t) \\ &= (1 + K_2)X_2(t) \\ &= \left(1 + \frac{1}{K_2}\right)X_3(t) \end{aligned} \tag{17}$$

we can eliminate X_2 and X_3 in favour of X_{23} to give the following reaction scheme:

$$\cdots X_1 \underset{\alpha_1^-}{\overset{\alpha_1^+}{\rightleftharpoons}} X_{23} \underset{\alpha_3^-}{\overset{\alpha_3^+}{\rightleftharpoons}} X_4 \cdots,$$

where the *apparent* rate constants, $\alpha_i^{\pm}$, are defined by

$$\begin{aligned} \alpha_1^+ &= k_1^+, \qquad \alpha_3^+ = \frac{k_3^+}{1 + 1/K_2}, \\ \alpha_1^- &= \frac{k_1^-}{1 + K_2}, \qquad \alpha_3^- = k_3^-. \end{aligned} \tag{18}$$

This simple lumping scheme is *proper*, i.e., formally equivalent to the full kinetic system, *only* in the limit of the rapid equilibrium approximation for X_2 and X_3. However, it is a reasonable approximation to make if the first-order forward and backward reaction rates of the fast reaction step are at least an order of magnitude greater than the rates of the other reaction steps.

3.2. Lumping and slow–fast kinetics

It is straightforward to show that the lumping scheme represents the slow subsystem of a slow–fast kinetic system. In such a system the variables evolve on one of two timescales. Fast variables rapidly approach an approximate steady-state, subsequently following the dynamics of the slow variables adiabatically. For the example above, focusing on the rapid reaction step:

$$\overset{J_{\text{in}}}{\rightarrow} X_2 \underset{k_2^-}{\overset{k_2^+}{\rightleftharpoons}} X_3 \overset{J_{\text{out}}}{\longrightarrow}$$

we can formally investigate this lumping scheme by writing the kinetic equations in terms of a small-valued parameter ε,

$$k_2^- = \frac{1}{\varepsilon}, \quad k_2^+ = \frac{K_2}{\varepsilon}, \quad 0 < \varepsilon \ll 1 \tag{19}$$

so that rate constants $k_2^+, k_2^- \gg 1$, and the equilibrium constant $K_2 \sim \mathcal{O}(1)$ (i.e., K_2 is of order unity). Then, with no approximation, we can write

$$\varepsilon \frac{\mathrm{d}X_2}{\mathrm{d}t} = \varepsilon J_{\text{in}} - K_2 X_2 + X_3, \tag{20}$$

$$\varepsilon \frac{\mathrm{d}X_3}{\mathrm{d}t} = K_2 X_2 - X_3 - \varepsilon J_{\text{out}}. \tag{21}$$

Substituting the new variable $X_{23} = X_2 + X_3$ in favour of X_3, we find

$$\varepsilon \frac{\mathrm{d}X_2}{\mathrm{d}t} = \varepsilon J_{\mathrm{in}} - K_2 X_2 + (X_{23} - X_2), \tag{22}$$

$$\frac{\mathrm{d}X_{23}}{\mathrm{d}t} = J_{\mathrm{in}} - J_{\mathrm{out}}. \tag{23}$$

We can rescale time to identify the dynamics on the fast timescale by writing $T = t/\varepsilon$ and then taking the limit as $\varepsilon \to 0$, giving

$$\frac{\mathrm{d}X_2}{\mathrm{d}T} \approx -K_2 X_2 + (X_{23} - X_2), \tag{24}$$

$$\frac{\mathrm{d}X_{23}}{\mathrm{d}T} \approx 0 \tag{25}$$

which is the fast subsystem, and so on the fast timescale X_2 approaches a steady-state $X_2 = X_{23}/(1 + K_2)$. Thus X_2 and X_3 rapidly approach their equilibrium concentration ratio $X_2 = X_3/K_2$, while the slow variable X_{23} remains approximately constant.

On the slow timescale, again taking the limit $\varepsilon \to 0$ for Eqs. (22) and (23), we find the slow subsystem is governed by

$$\frac{\mathrm{d}X_{23}}{\mathrm{d}t} \approx J_{\mathrm{in}} - J_{\mathrm{out}}, \tag{26}$$

$$X_2 \approx \frac{X_{23}}{1 + K_2}. \tag{27}$$

Hence the rapid equilibrium approximation for X_2 and X_3 is simply the leading order asymptotic expression in the limit as $\varepsilon \to 0$, exploiting slow and fast timescales in the model.

This approach can be extended to any number of sequential reaction steps at rapid equilibrium, and applies equally to partial reactions that make up a reaction cycle, as for the sodium–potassium pump. In general, for n consecutive partial reactions at rapid equilibrium there will be n fast variables and one lumped slow variable which is the sum of $n + 1$ enzyme states:

$$\cdots \underset{k_{i-1}^-}{\overset{k_{i-1}^+}{\rightleftharpoons}} X_i \overset{K_i}{\rightleftharpoons} X_{i+1} \overset{K_{i+1}}{\rightleftharpoons} X_{i+2} \rightleftharpoons \cdots \rightleftharpoons X_{i+n} \underset{k_{i+n}^-}{\overset{k_{i+n}^+}{\rightleftharpoons}} \cdots,$$

where $K_i = k_i^+/k_i^-$ is the equilibrium constant (in the forward direction), denoting the ith rapid equilibrium reaction. The reduction of the kinetics to a single lumped variable X_{Σ_i}

$$X_{\Sigma_i}(t) = \sum_{j=0}^{n} X_{i+j}(t) \tag{28}$$

so that the sequence of equilibrium reactions is approximated by the scheme

$$\cdots X_{i-1} \underset{\alpha_{i-1}^-}{\overset{\alpha_{i-1}^+}{\rightleftharpoons}} X_{\Sigma_i} \underset{\alpha_{i+n}^-}{\overset{\alpha_{i+n}^+}{\rightleftharpoons}} X_{i+n+1} \cdots,$$

where

$$\alpha^+_{i-1} = k^+_{i-1}, \qquad \alpha^+_{i+n} = \frac{k^+_{i+n}\prod_{s=i}^{i+n-1} K_s}{1+\sum_{r=1}^{n}\prod_{s=i}^{i+r-1} K_s},$$
$$\alpha^-_{i-1} = \frac{k^-_{i-1}}{1+\sum_{r=1}^{n}\prod_{s=i}^{i+r-1} K_s}, \qquad \alpha^-_{i+n} = k^-_{i+n}. \tag{29}$$

Although these expressions appear complicated, their use considerably simplifies the reaction diagram to be analysed.

3.3. Rapid equilibrium partial reactions for Na/K-ATPase

Application of the reduction technique based on slow and fast timescales outlined above allows a dramatic simplification of the dynamics underlying the Post-Albers cycle for the Na/K-ATPase, due to the number of partial reactions which can be considered to be at rapid equilibrium. Lumping the states in rapid equilibrium produces the state diagram shown in Fig. 2. We will define the forward cycle direction to be represented by clockwise paths in diagrams, and by rate constants k^+. Equilibrium constants are then the ratio of forward (clockwise) to backward (anti-clockwise) rate constants, k^+/k^-, as before. From the above analysis the apparent transition rates between the lumped states in Fig. 2 are easily calculated. For the forward reaction steps:

$$\alpha^+_1 = \frac{k^+_1 \widetilde{\mathrm{Na_i}}^3}{(1+\widetilde{\mathrm{Na_i}})^3+(1+\widetilde{\mathrm{K_i}})^2-1}, \qquad \alpha^+_2 = k^+_2,$$
$$\alpha^+_3 = \frac{k^+_3 \widetilde{\mathrm{K_e}}^2}{(1+\widetilde{\mathrm{Na_e}})^3+(1+\widetilde{\mathrm{K_e}})^2-1}, \qquad \alpha^+_4 = \frac{k^+_4 \widetilde{\mathrm{MgATP}}}{1+\widetilde{\mathrm{MgATP}}} \tag{30}$$

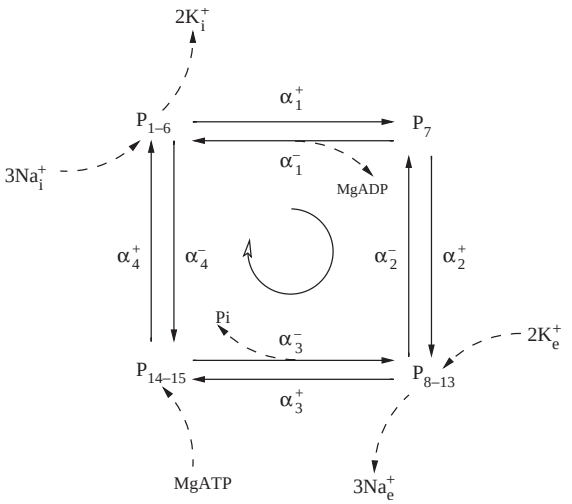

Fig. 2. The reduced scheme for the Na/K-ATPase. Pseudo-first-order rate constants $\alpha_j^{\pm}$ incorporate the ion and metabolite binding and unbinding reactions (dotted arrows).

and for the reverse:

$$\alpha_1^- = k_1^- [\mathrm{MgADP}], \qquad \alpha_2^- = \frac{k_2^- \widetilde{\mathrm{Na}}_\mathrm{e}^3}{(1+\widetilde{\mathrm{Na}}_\mathrm{e})^3 + (1+\widetilde{\mathrm{K}}_\mathrm{e})^2 - 1},$$
$$\alpha_3^- = \frac{k_3^- [\mathrm{Pi}][\mathrm{H}^+]}{1+\widetilde{\mathrm{MgATP}}}, \qquad \alpha_4^- = \frac{k_4^- \widetilde{\mathrm{K}}_\mathrm{i}^2}{(1+\widetilde{\mathrm{Na}}_\mathrm{i})^3 + (1+\widetilde{\mathrm{K}}_\mathrm{i})^2 - 1}, \tag{31}$$

where

$$\widetilde{\mathrm{Na}}_\mathrm{i} = \frac{[\mathrm{Na_i}]}{K_{\mathrm{d},Na_\mathrm{i}}}, \qquad \widetilde{\mathrm{K}}_\mathrm{i} = \frac{[\mathrm{K_i}]}{K_{\mathrm{d},K_\mathrm{i}}}, \qquad \widetilde{\mathrm{MgATP}} = \frac{[\mathrm{MgATP}]}{K_{\mathrm{d,MgATP}}},$$
$$\widetilde{\mathrm{Na}}_\mathrm{e} = \frac{[\mathrm{Na_e}]}{K_{\mathrm{d},Na_\mathrm{e}}} \qquad \widetilde{\mathrm{K}}_\mathrm{e} = \frac{[\mathrm{K_e}]}{K_{\mathrm{d},K_\mathrm{e}}} \tag{32}$$

and K_d are the dissociation constants for ion binding and where the voltage dependence is through the dissociation constants for sodium ions. Transition rates α_i^+ are in the forward, clockwise direction, and α_i^- in the reverse (anti-clockwise) direction. Thus we see that the kinetics of this pump are in fact fully determined by eight *non-independent* parameters.

In their earlier model of the sodium–potassium pump, Chapman et al. (1979) considered a rate expression for the net reaction, Eq. (1), for which they needed to include an explicit empirical concentration dependence as well as voltage dependence for the forward and backward reaction rates. In the reduced model presented here, based on the Post-Albers scheme, the dependence of the rate expressions on intra and extracellular ion concentrations comes through the sequential binding and unbinding steps in the reaction cycle only.

As noted above, the expression for α_3^- must also account for the equilibrium between free inorganic phosphate [Pi] and its bound species [HPi], [KPi] and [NaPi]. Assuming rapid buffering, each of these species is at equilibrium with Pi, and the free inorganic phosphate concentration is related to the total *measurable* concentration, [ΣPi], via

$$[\Sigma\mathrm{Pi}] = [\mathrm{Pi}] + [\mathrm{KPi}] + [\mathrm{NaPi}] + [\mathrm{HPi}] = [\mathrm{Pi}]\left(1 + \frac{[\mathrm{K_i}]}{K_{\mathrm{d,KPi}}} + \frac{[\mathrm{H}]}{K_{\mathrm{d,HPi}}} + \frac{[\mathrm{Na_i}]}{K_{\mathrm{d,NaPi}}}\right).$$

Thus the [Pi] term should be replaced by

$$[\mathrm{Pi}] = \frac{[\Sigma\mathrm{Pi}]}{(1 + [\mathrm{K_i}]/K_{\mathrm{d,KPi}} + [\mathrm{H}]/K_{\mathrm{d,HPi}} + [\mathrm{Na_i}]/K_{\mathrm{d,NaPi}})}, \tag{33}$$

where [ΣPi] is the total concentration of inorganic phosphate as measured, for example, by NMR experiment.

3.4. Quasi-steady-state pump velocity

The general approach for whole-cell modelling of pump kinetics is to assume that the pump operates at a kinetic steady-state. This is different to the rapid equilibrium approximation made above for individual reaction steps: if all partial reactions in the diagram were at equilibrium there would be no net flux around the cycle and hence no transport of ions (i.e., thermodynamic equilibrium). The quasi-steady-state approximation assumes that the conformational changes of the enzyme and other associated events are rapid compared to slower processes of interest in the

cell, for example, changes to ionic concentrations. This again is a simplification based on difference of timescales, and can be formalised in terms of slow–fast kinetics.

For a simple cycle with no branching, at steady-state the flux through any of the different enzyme forms, or states of the model, must be the same. Because the interaction between states in the diagram is linear in the state occupancy probabilities, that is, transitions from one state to another depend only the probability of being in that state in the first place, the steady-state rate expressions form a linear algebraic system of equations. The steady-state flux can be calculated, for example, for cyclical reaction schemes using the diagrammatic King-Altman-Hill approach (King and Altman, 1956; Hill, 1996, 1989), and in particular its algorithmic implementation (Cornish-Bowden, 1977; Mulquiney and Kuchel, 2003). Essentially these techniques amount to the solution of the linear algebraic system for the steady-state probabilities.

For the simplified model of the Na/K-ATPase, conservation of the total amount of enzyme reduces the steady-state equations to a system of three coupled linear algebraic equations. As described above, this system can be solved for the steady-state cycle rate by (i) solving the equations directly or (ii) using the diagram method. The clockwise rate v_{cyc} at steady-state is given by

$$v_{\mathrm{cyc,Na/K}} = \frac{\alpha_1^+\alpha_2^+\alpha_3^+\alpha_4^+ - \alpha_1^-\alpha_2^-\alpha_3^-\alpha_4^-}{\Sigma}, \tag{34}$$

where Σ, in this case, is a sum of 16 positive product terms (from the diagram method, the sum of the directional diagrams for all four states—see Hill, 1989), and is easily calculated. The whole-cell pump current density $i_{\mathrm{Na/K}}$ is then given by

$$i_{\mathrm{Na/K}} = v_{\mathrm{cyc,Na/K}}\, F \rho_{\mathrm{Na/K}}, \tag{35}$$

where $\rho_{\mathrm{Na/K}}$ is the density of Na/K-ATPase proteins in the sarcolemma.

What remains to be done in this study is to determine the rate constants $k_i^{\pm}$, $i = 1, \ldots, 4$, dissociation constants $K^0_{\mathrm{d,Na_i}}$, $K^0_{\mathrm{d,Na_e}}$, $K_{\mathrm{d,K_i}}$, $K_{\mathrm{d,K_e}}$, $K_{\mathrm{d,MgATP}}$ and voltage-dependence partition factor Δ from experimental data in the literature, and hence determine the eight parameter groupings for the reduced model. This is carried out in the following section.

4. Fitting model parameters

The final step in model characterisation is the determination of parameters for the rate constants $k_j^{\pm}$ and equilibrium and dissociation constants in Eqs. (13) and (14), and hence parameter groupings $\alpha_j^{\pm}$ in Eq. (34). Initial guesses for these constants are the parameter values proposed by Läuger and Apell (1986). We have adjusted their parameters to remove implicit metabolite and proton concentrations, and increased the value of the equilibrium constant for MgATP, which was arbitrarily set in their model. Furthermore, we have chosen to specify k_1^- in terms of the other parameters using Eq. (13) for thermodynamic consistency and therefore we have recalculated k_1^- for this initial parameter set. The standard free energy of MgATP hydrolysis $\Delta G^o_{\sim \mathrm{MgATP}} = -29.6$ kJ mol^{-1} (Guynn and Veech, 1973) was calculated from the equilibrium concentrations of metabolites (via the equilibrium constant $K_{\sim \mathrm{MgATP}}$) according to Eq. (4). After these modifications, we have also increased the values of the rate constants in the initial parameter set by a factor of 4 to account for the change from 298 K (25°C), the temperature at which the

Table 1
The initial estimates (left-hand column) and final fitted values (right-hand column) for kinetic parameters for the sodium–potassium pump model shown in Fig. 2

Parameter	Initial estimates	Fitted value
k_1^+	1080 s^{-1}	1050 s^{-1}
k_1^-	80.0 s^{-1} mM^{-1}	172.1 $s^{-1}mM^{-1}$
k_2^+	480.0 s^{-1}	481.0 s^{-1}
k_2^-	40.0 s^{-1}	40.0 s^{-1}
k_3^+	2000 s^{-1}	2000 s^{-1}
k_3^-	400.0×10^6 $s^{-1}mM^{-2}$	79.3×10^3 $s^{-1}mM^{-2}$
k_4^+	320.0 s^{-1}	320.0 s^{-1}
k_4^-	40.0 s^{-1}	40.0 s^{-1}
K^0_{d,Na_e}	100.0 mM	15.5 mM
K^0_{d,Na_i}	4.0 mM	2.49 mM
K_{d,K_e}	2.0 mM	0.213 mM
K_{d,K_i}	8.0 mM	0.500 mM
$K_{d,MgATP}$	6.0 mM	2.51 mM
Δ	−0.3	−0.031

experiments were performed, to 310 K (37°C) corresponding to a Q_{10} of 3.2 (Läuger and Apell, 1986). The initial set of parameter values is shown in Table 1.

The model parameters were estimated using a sequential quadratic programming algorithm (Fletcher, 1987). This method allows a priori upper and lower bounds to be placed on each of the parameters, and was found to converge to a minimising solution more reliably than full line searching along the direction of steepest descent. The residual errors were calculated from the model using the current–voltage data of Nakao and Gadsby (1989) (reproduced in Fig. 3) who measured pump turnover rate as a function of transmembrane voltage for four different levels of extracellular sodium. The model results using the parameter set in the right-hand column of Table 1 are shown in Fig. 3 where, for comparison, the original data and an empirical curve fit to the data by Nakao and Gadsby are also reproduced. The maximum pump cycling rate of 55 s^{-1} with a cell membrane pump density $\rho_{Na/K} = 2200$ μm^{-2} for guinea pig ventricular myocytes (Kockskamper et al., 2000), is consistent with a maximal pump current, $i_{Na/K}$, of 1.9 μA cm^{-2} (Gray et al., 1997).

While one must be cautious about drawing definitive conclusions regarding fitted parameter values for large parameter sets, it is interesting to note the large changes in the rate parameters k_1^- and k_3^- and in the dissociation constants (in Table 1) resulting from the fitting process. The temperature adjusted value of k_1^- proposed by Läuger and Apell (1986) is 80 s^{-1} mM^{-1}, however, to enforce thermodynamic consistency k_1^- was calculated using Eq. (13) to give a fitted value of 172.1 s^{-1} mM^{-1}. Despite the changes, these values are still consistent with the relatively wide range of experimental estimates in the literature for rate parameters (Glitsch, 2001) and dissociation constants, which, one study has recently suggested, may in some cases also show dependence on intracellular pH (Apell and Diller, 2002).

4.1. Energetic consequences of raised intracellular sodium concentration

The model has been used (Fig. 4(a)) to demonstrate the energetic relationship between $\Delta G_{\sim MgATP}$ and the pump cycle rate at different levels of intracellular sodium $[Na_i^+]$. To simulate

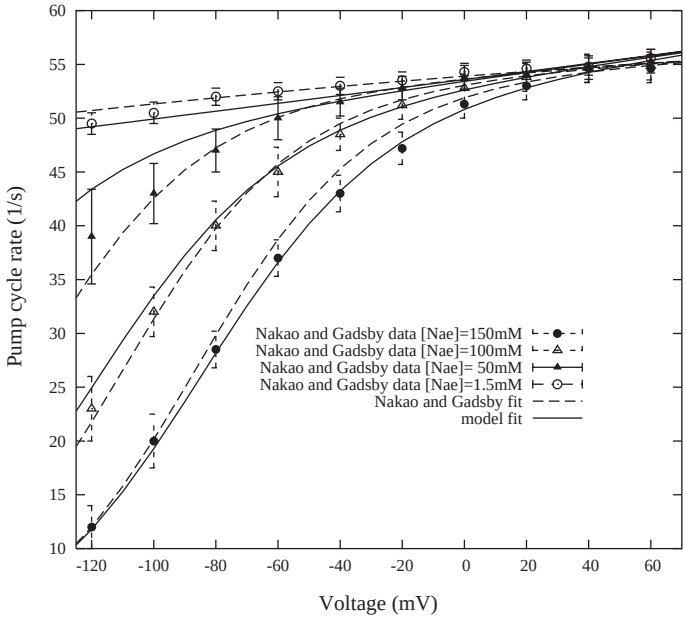

Fig. 3. The data of Nakao and Gadsby (1989), their empirical fit (R.M.S. error 1.52 s^{-1}) and the reduced model fit (R.M.S. error 1.71 s^{-1}) for pump cycling rate vs. voltage for different values of $[Na_e^+]$. To be consistent with the study by Nakao and Gadsby (1989), other ionic concentrations are $[Na_i^+] = 50$ mM, $[K_e^+] = 5.4$ mM and $[K_i^+] = 140$ mM; [MgATP] = 9.8 mM, [MgADP] = 0.05 mM, [ΣPi] = 4.2 mM and pH = 7; temperature $T = 310$ K; and constants: $R = 8.314$ J mol^{-1} K^{-1}, $F = 96.485 \times 10^3$ C mol^{-1}, and dissociation constants for inorganic phosphate $pK_{d,HPi} = 6.77$, $K_{d,KPi} = 292$ mM and $K_{d,NaPi} = 224$ mM (Smith and Alberty, 1956; Lawson and Veech, 1979).

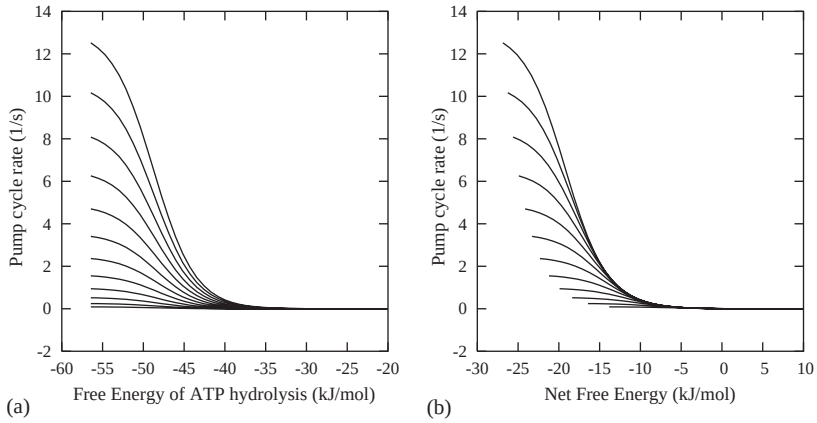

Fig. 4. The influence of intracellular sodium concentration, $[Na_i^+]$, and free energy of ATP hydrolysis on pump cycling rate at constant transmembrane voltage. (a) Change in pump cycling rate as a function of $\Delta G_{\sim MgATP}$ for different concentrations of $[Na_i^+]$: for the lowest curve $[Na_i^+] = 5$ mM, increasing by 2 mM for each subsequent curve up to 29 mM for the top curve. (b) The same curves plotted against net free energy change $\Delta G_{\sim MgATP} + \Delta G_{pump}$. The other concentrations are $[Na_e^+] = 150$ mM, $[K_e^+] = 5.4$ mM, $[K_i^+] = 140$ mM, [MgATP] = 9.8 mM, [ΣPi] = 4.2 mM, pH = 7 and transmembrane voltage $V_m = -85$ mV. Following Spindler et al. (2002), the free energy change is brought about by varying [MgADP].

the effect of ischaemia in the myocyte the concentration of intracellular MgADP was progressively increased (Spindler et al., 2002). This rise in concentration of hydrolysis products reduces the free energy available from MgATP hydrolysis, and results in a drop in pump cycle rate for a given level of intracellular sodium. Increasing the level of intracellular sodium produces a decrease in the free energy required for the pump to cycle, $|\Delta G_{\text{pump}}|$. This is manifested by the pump reaching thermodynamic equilibrium, i.e., zero cycle rate, at a less negative hydrolysis free energy. These results are consistent with the results of Jansen et al. (2003) who show that the rise in intracellular sodium partially offsets the reduction in free energy available from MgATP hydrolysis under ischaemic conditions. Figure 4(b) confirms the thermodynamic properties of the model, plotting the same relationship against the net free energy of a pump cycle ($\Delta G_{\sim \text{MgATP}} + \Delta G_{\text{pump}}$). In this graph, we see that pump cycling stops across all concentrations of intracellular sodium when the net free energy of the system approaches zero. As is evident from the figure, with this set of kinetic parameters the pump reversal current is negligible at positive free energies, which is also consistent with the findings of Jansen et al. (2003). By suitably increasing [MgATP], $[Na_e^+]$ or $[K_i^+]$, and reducing $[K_e^+]$, for example, the pump can be made to run in reverse at an appreciable rate, transporting Na^+ into the cell, generating a net inward current.

5. Discussion

Understanding the catalytic properties of proteins, from sequence data through protein structure to kinetics and function, is a highly complicated and multiscaled problem (Fersht, 1999). Retaining the biophysical properties of pumps for whole-cell modelling provides a number of benefits for ongoing model development. First, it ensures a transparent link between model and data—both to existing data and new experimental results. This provides the potential for accelerated understanding via the iteration between experimental study and computational analysis, which adds considerably to the knowledge to be gained from either exercise alone (Noble, 2002b). A second advantage is the maintenance of the model as an extensible framework, with the ability to incorporate data from novel experimental techniques and to simulate additional pathologies. The model 'upgrade path' is more readily apparent as new data become available, increasing the return on the initial modelling effort (Noble, 2002a). A further advantage of a biophysically based modelling approach, rather than one based solely on empirical relationships determined by fitting curves to experimental data, is in providing some confidence in the properties of the model when extrapolated outside the range of the data used in parameter estimation. It is in this potential for extrapolation, in addition to the interpolation of experimental data, that the great strength of the modelling and simulation of physiological systems resides.

We have looked at a lumping scheme which is based on rapid equilibrium reactions, and have shown that it is formally consistent with leading order asymptotic expressions for kinetics with slow–fast separation of timescales. In the case of the Na/K-ATPase, we have been able to reduce the enzymatic cycle down to a 4-state model, which is more readily analysed and, crucially, which retains the thermodynamic consistency of the more complex representation of the enzymatic cycle. The effectiveness for computational simulation studies of any model reduction method, including the one proposed in this study, should be measured against two criteria. The first is how well the model fit to experimental data is maintained after the simplification steps, and the second criterion

is the computation time saved following the model reduction. The reduction method developed in this study eliminates one parameter, a fast relative reaction timescale (ε in Eq. (19)), for *each* rapid equilibrium reaction, so that these reactions are represented in the reduced model as a single equilibrium or dissociation constant. In the model reduction, five parameters are removed by assuming that each ligand binding can be represented as an equilibrium step. This rapid equilibrium assumption is generally well supported by experimental evidence (Kane et al., 1997; Cornelius, 1999). The extent to which the fit in Fig. 3 is compromised by this assumption was assessed by reintroducing explicit forward and backward rate constants for each equilibrium reaction (i.e., choosing a value for ε for each of these reactions) and repeating the fitting process. This produced a small reduction in the root mean-squared error as would be expected (from 1.71 to 1.48 s^{-1}), however, the fit to data for the reduced model is already within the experimental error, making it difficult to justify inclusion of these ion binding rate constants which in any case, to our knowledge, have not yet successfully been measured.

The second criterion of improvement to computation times also depends on the magnitude of the forward and backward reaction rate constants for the ligand binding steps. To determine the probable computational gain we have performed simulations of the full model choosing the rate constants to be an order of magnitude larger than the next fastest transition rate in the full model. Measuring the computational time taken to simulate the model kinetics over a 100 ms period following a step change in membrane voltage from -80 to -60 mV we have found an approximately 10-fold reduction in computational load for the reduced model. This is largely due to the fact that the fast transition rates for the full model give rise to a highly stiff system of ordinary differential equations, and even with the use of specially adapted integration techniques such as the method of Gear (1971), the stiff system is more computationally intensive to solve. For faster rapid binding rates we have found that the increase in computational time required to solve the full model as $1/\varepsilon$ increases is approximately linear.

The principles which have been employed for this enzyme are straightforward to apply to the other ATPases in the myocyte. Although the Post-Albers pump cycle for the Na/K-ATPase, which is analysed above, is a simple enzymatic cycle with no branching, or slippage, the simplification steps which we have highlighted can be applied to any reaction mechanism or set of partial reaction steps. The slow–fast timescales analysis used to justify the lumping scheme was made on the basis that a fast reaction could be considered to equilibrate rapidly. For several partial reactions operating on the same fast timescale, each can be considered to equilibrate on the same fast timescale. In general, when there are partial reactions with a range of timescales, then any division into a set of slow and a set of fast reactions, sufficiently separated in timescales (by an order of magnitude or more), can give rise to the same lumping scheme and model reduction approach. Other situations where simple paths to model reduction arise include the case for which certain states of the enzyme are only marginally occupied, as for example due to very large input and output kinetic parameters (in contrast to the fast forward and backward reaction rates for a particular reaction step, which we have analysed in this paper). These and other situations are also formally dealt with by the slow–fast approach outlined above. Similarly, the thermodynamic considerations which are outlined are universal, although they may be more complicated in form for more complicated kinetic schemes.

The goal of this research is to build comprehensive models of cardiac myocyte metabolism. In the ischaemic heart the supply of metabolic substrates to ATP-hydrolysing ion pumps is reduced,

leading to gross disturbances to their function which, along with many other changes to the normal ionic homeostasis, can cause severe disruption to the normal electrical and contractile function of the cell. To this end, we are currently undertaking a similar approach for other active components of the excitation-contraction coupling apparatus in the cardiac cell, along with explicit consideration of pH effects on these enzymes. Models of these individual components that retain details of the underlying molecular processes which regulate their kinetics will be of great importance to attempts to understand the progressive changes during ischaemic disease.

Acknowledgements

NPS acknowledges funding from the New Zealand Institute of Mathematics and its Applications (NZIMA) and the Royal Society of New Zealand. EJC acknowledges support from the Wellcome Trust, and thanks Prof. Peter Hunter and the Bioengineering Institute, University of Auckland. Both authors would also like to thank Dr. Peter Mulquiney.

References

Apell, H.J., 1989. Electrogenic properties of the Na,K pump. J. Membr. Biol. 110, 103–114.

Apell, H.J., Diller, A., 2002. Do H^+ ions obscure electrogenic Na^+ and K^+ binding in the E_1 state of the Na,K-ATPase? FEBS Lett. 532 (1–2), 198–202.

Chapman, J.B., Kootsey, J.M., Johnson, E.A., 1979. A kinetic model for determining the consequences of electrogenic active transport in cardiac muscle. J. Theor. Biol. 80, 405–424.

Ch'en, F.F.T., Vaughan-Jones, R.D., Clark, K., Noble, D., 1998. Modelling myocardial ischaemia and reperfusion. Prog. Biophys. Mol. Biol. 69, 497–515.

Cornelius, F., 1999. Rate determination in phosphorylation of shark rectal Na,K-ATPase by ATP: temperature sensitivity and effects of ADP. Biophys. J. 77 (2), 934–942.

Cornish-Bowden, A., 1977. An automatic method for deriving steady-state rate equations. Biochem. J. 165, 55–59.

De Weer, P., Gadsby, D.C., Rakowski, R.F., 1988. Voltage dependence of the Na–K pump. Annu. Rev. Physiol. 50, 225–241.

Fell, D.A., 1997. Understanding the Control of Metabolism. Portland Press, London.

Fersht, A., 1999. Structure and Mechanism in Protein Science: A Guide to Enzyme Catalysis and Protein Folding. Freeman and Co., New York.

Fletcher, R., 1987. Practical Methods of Optimization, 2nd Edition. Wiley, New York.

Gear, C.W., 1971. The automatic integration of ordinary differential equations. Commun. ACM 14, 176–179.

Glitsch, H.G., 2001. Electrophysiology of the sodium-potassium-ATPase in cardiac cells. Physiol Rev. 81 (4), 1791–1826.

Glitsch, H.G., Tappe, A., 1995. Change of Na^+ pump current reversal potential in sheep cardiac purkinje-cells with varying free-energy of ATP hydrolysis. J. Physiol. 484, 605–616.

Glynn, I.M., Lew, V.L., 1970. Synthesis of adenosine triphosphate at the expense of downhill cation movements in intact human red cells. J. Physiol. 207, 393–402.

Gray, D.F., Hansen, P.S., Doohan, M.M., Hool, L.C., Rasmussen, H.H., 1997. Dietary cholesterol affects Na^+–K^+ pump function in rabbit cardiac myocytes. Am. J. Physiol. 272 (4), H1680–H1689.

Gupta, R.K., Benovic, J.L., Rose, Z.B., 1978. The determination of the free magnesium level in the human red blood cell by 31P NMR. J. Biol. Chem. 253 (17), 6172–6176.

Guynn, R.W., Veech, R.L., 1973. The equilibrium constants of the adenosine triphosphate hydrolysis and the adenosine triphosphate-citrate lyase reactions. J. Biol. Chem. 248 (20), 6966–6972.

Hill, T.L., 1989. Free Energy Transduction and Biochemical Cycle Kinetics. Springer, New York.

Hill, T.L., 1996. Studies in irreversible thermodynamics IV. Diagrammatic representation of steady state fluxes for unimolecular systems. J. Theor. Biol. 10, 422–459.

Huang, W.-H., Askari, A., 1984. Regulation of Na^+–K^+-ATPase by inorganic-phosphate—pH-dependence and physiological implications. Biochem. Biophys. Res. Commun. 123, 438–443.

Ingwall, J.S., 2002. ATP and the Heart. Kluwer Academic Publishers, Dordrecht.

Jansen, M.A., Shen, H., Zhang, L., Wolkowicz, P.E., Balschi, J.A., 2003. Energy requirements for the Na^+ gradient in the oxygenated isolated heart: effect of changing the free energy of ATP hydrolysis. Am. J. Physiol. 285, H2437–H2445.

Johnson, E.A., Chapman, J.B., Kootsey, J.M., 1980. Some electrophysiological consequences of electrogenic sodium and potassium transport in cardiac muscle: a theoretical study. J. Theor. Biol. 87, 737–756.

Kane, D.J., Fendler, K., Grell, E., Bamberg, E., Taniguchi, K., Froehlich, J.P., Clarke, R.J., 1997. Stopped-flow kinetic investigations of conformational changes of pig kidney Na^+, K^+-ATPase. Biochemistry 36 (43), 13406–13420.

King, E.L., Altman, C., 1956. A schematic method of deriving the rate laws for enzyme-catalyzed reactions. J. Phys. Chem. 60, 1375–1378.

Kockskamper, J., Erlenkamp, S., Glitsch, H.G., 2000. Activation of the cAMP-protein kinase A pathway facilitates Na^+ translocation by the Na^+–K^+ pump in guinea-pig ventricular myocytes. J. Physiol. 523, 561–574.

Läuger, P., Apell, H.J., 1986. A microscopic model for the current–voltage behaviour of the Na,K-pump. Eur. Biophys. J. 13, 309–321.

Lawson, J.W.R., Veech, R.L., 1979. Effects of pH and free Mg^{2+} on the K_{eq} of the creatine kinase reaction and other phosphate hydrolysis and phosphate transfer reactions. J. Biol. Chem. 254, 6528–6537.

Lew, V.L., Glynn, I.M., Ellory, J.C., 1970. Net synthesis of ATP by reversal of the sodium pump. Nature 225, 865–866.

Luo, C., Rudy, Y., 1994a. A dynamic model of the cardiac ventricular action potential: I. Simulations of ionic currents and concentration changes. Circ. Res. 74 (6), 1071–1096.

Luo, C., Rudy, Y., 1994b. A dynamic model of the cardiac ventricular action potential: II. After depolarizations, triggered activity, and potentiation. Circ. Res. 74 (6), 1097–1113.

Mulquiney, P.J., Kuchel, P.W., 2003. Modelling Metabolism with Mathematica. CRC Press, Doca Raton, FL.

Nakao, M., Gadsby, D.C., 1989. [Na] and [K] dependence of the Na/K pump current–voltage relationship in guinea-pig ventricular myocytes. J. Gen. Physiol. 94, 539–565.

Noble, D., 2002a. Modeling the heart from genes to cells to the whole organ. Science 5560 (295), 1678–1682.

Noble, D., 2002b. The rise of computational biology. Nat. Rev. Mol. Cell Biol. 3 (6), 459–463.

Noble, D., Rudy, Y., 2001. Models of cardiac ventricular action potentials: iterative interaction between experiment and simulation. Philos. Trans. R. Soc. London Ser. A. 359, 1127–1142.

Noble, D., Varghese, A., Kohl, P., Noble, P., 1998. Improved guinea-pig ventricular model incorporating diadic space, i_{kr} and i_{ks}, length and tension-dependent processes. Can. J. Cardiol. 14, 123–134.

Rakowski, R.F., Bezanilla, F., De Weer, P., Gadsby, D.C., Holmgren, M., Wagg, J., 1997. Charge translocation by the Na/K pump. Ann. N. Y. Acad. Sci. 834, 231–243.

Schramm, M., Klieber, H.G., Daut, J., 1994. The energy expenditure of actomyosin-ATPase, Ca^{2+}-ATPase and Na^+, K^+-ATPase in guinea-pig cardiac ventricular muscle. J. Physiol. 481, 647–662.

Skou, J.C., 1957. The influence of some cations on an adenosine triphosphatase from peripheral nerves. Biochim. Biophys. Acta 23, 394–401.

Smith, R.M., Alberty, R.A., 1956. The apparent stability constants of ionic complexes of various adenosine phosphates with monovalent cations. J. Phys. Chem. 60, 180–184.

Spindler, M., Niebler, R., Remkes, H., Horn, M., Lanz, T., Neubauer, S.M., 2002. Mitochondrial creatine kinase is critically necessary for normal myocardial high-energy phosphate metabolism. Am. J. Physiol. 283 (2), H680–H687.

Tanford, C., 1981. Equilibrium state of ATP-driven ion pumps in relation to physiological ion concentration gradients. J. Gen. Physiol. 77, 223–229.

Toyoshima, C., Nakasako, M., Nomura, H., Ogawa, H., 2000. Crystal structure of the calcium pump of sarcoplasmic reticulum at 2.6 angstrom resolution. Nature 405, 647–655.